

1  
2  
3  
4       Whole brain comparative anatomy using connectivity blueprints  
5  
6  
7  
8  
9

10       Rogier B. Mars<sup>1,2,\*</sup>, Stamatis N. Sotiropoulos<sup>1,3</sup>, Richard E. Passingham<sup>4</sup>,  
11       Jerome Sallet<sup>4</sup>, Lennart Verhagen<sup>4</sup>, Alexandre A. Khrapitchev<sup>5</sup>, Nicola Sibson<sup>5</sup>,  
12       and Saad Jbabdi<sup>1,\*</sup>  
13  
14  
15  
16

17       <sup>1</sup>Wellcome Centre for Integrative Neuroimaging, Centre for Functional MRI of the  
18       Brain (FMRIB), Nuffield Department of Clinical Neurosciences, John Radcliffe  
19       Hospital, University of Oxford, Oxford, United Kingdom

20       <sup>2</sup>Donders Institute for Brain, Cognition and Behaviour, Radboud University Nijmegen,  
21       Nijmegen, The Netherlands

22       <sup>3</sup>Sir Peter Mansfield Imaging Centre, School of Medicine, University of Nottingham,  
23       Nottingham, United Kingdom

24       <sup>4</sup>Department of Experimental Psychology, University of Oxford, Tinbergen Building,  
25       South Parks Road, Oxford OX1 3UD, United Kingdom

26       <sup>5</sup>Cancer Research UK and Medical Research Council Oxford Institute for Radiation  
27       Oncology, Department of Oncology, University of Oxford, Oxford, United Kingdom

30       Abbreviated title: The primate connectivity blueprint  
31  
32  
33  
34  
35

36       \*Correspondence:

37       Rogier B. Mars and Saad Jbabdi

38       Centre for Functional MRI of the Brain (FMRIB)

39       Nuffield Department of Clinical Neurosciences

40       John Radcliffe Hospital

41       University of Oxford

42       Oxford OX3 9DU

43       United Kingdom

44       E-mail: [rogier.mars@ndcn.ox.ac.uk](mailto:rogier.mars@ndcn.ox.ac.uk) and [saad@fmrib.ox.ac.uk](mailto:saad@fmrib.ox.ac.uk)

45

46

47

48 **Abstract**

49

50 Comparing the brains of related species faces the challenges of establishing  
51 homologies whilst accommodating evolutionary specializations. Here we propose a  
52 general framework for understanding similarities and differences between the brains  
53 of primates. The approach uses white matter blueprints of the whole cortex based  
54 on a set of white matter tracts that can be anatomically matched across species. The  
55 blueprints provide a common reference space that allows us to navigate between  
56 brains of different species, identify homologous cortical areas, or to transform whole  
57 cortical maps from one species to the other. Specializations are cast within this  
58 framework as deviations between the species' blueprints. We illustrate how this  
59 approach can be used to compare human and macaque brains.

60

61

62

63 **MAIN TEXT (2000-4000 words, excl online methods, references, and figure legends)**

64

65 The ultimate goal of comparative and evolutionary neuroscience is to understand  
66 the organization of each species' brain as an adaptation to its unique ecological  
67 niche. However, the study of specific adaptations cannot be performed without an  
68 appreciation of the common organizational principles of different brains. To  
69 understand what is unique about the brain of a given species, a useful starting point  
70 is to cast it in the context of a common template. Unique properties and adaptations  
71 of a species' brain can then be understood as deviations from the template.

72

73 In higher primates, white matter organization has striking commonalities between  
74 the different species (Thiebaut de Schotten et al. 2012). Several association  
75 pathways have been identified in humans, chimpanzees, and macaques (Rilling et al.  
76 2008, Hecht et al. 2013). These pathways share core properties such as the broad  
77 brain areas that they connect, but differ in the details of their branching patterns,  
78 suggesting a common connectivity backbone with varying degrees of connectivity  
79 specialization. We propose that common white matter pathways can be used to  
80 form *blueprints* of cortical connections to enable comparisons of cortical areas  
81 between higher primates.

82

83 We exploit the idea that cortical regions can be described by their unique sets of  
84 connections to the rest of the brain (Passingham et al. 2002), a feature that we have  
85 previously shown is useful in comparing brain organization between species (Mars et  
86 al. 2016). Thus, we can investigate neural organization using the architecture of the  
87 main white matter fibers. **The bodies of the major fiber bundles can be identified  
88 reliably in different species and allow identification of homologous fiber bundles.  
89 This allowed us to construct a map of each of the main white matter tracts and to  
90 describe cortical grey matter organization in terms of this map (Fig. 1). We term  
91 the matrix describing the connectivity of each vertex of the grey matter surface  
92 with each white matter tract the connectivity blueprint.** These connectivity  
93 blueprints provide a common space in which we can ask how each part of the grey  
94 matter in one species maps onto the other species.

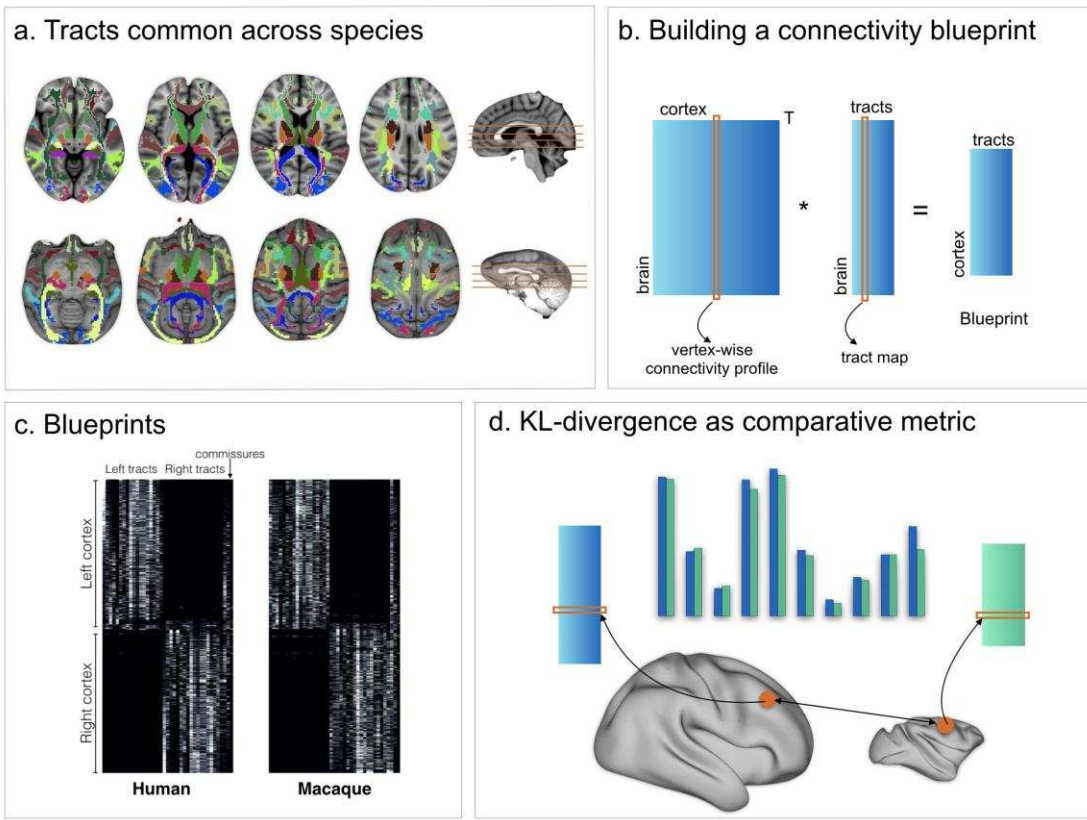
95

96 We illustrate this approach by comparing human and macaque cortex. We  
97 demonstrate that the connectivity blueprints can be used to predict the location of  
98 cortical areas across species. Furthermore, by quantifying the distances between the  
99 blueprints of different parts of the two brains, we quantify where these brains have  
100 tended to specialize since their last common ancestor. **We demonstrate that such  
101 areas overlap with known specializations in the human and macaque lineages.**

102

103 Our results show how connectivity blueprints can be used for comparative anatomy  
104 of humans and macaques, but the approach can be generalized to all higher  
105 primates where the blueprints can be identified. This method thus provides a  
106 powerful approach to comparative anatomy, and allows one to quantitatively define  
107 common principles and unique specializations in the brains of related animals.

108



109  
110 **Figure 1. Methods overview.** (a) 39 tracts common across both species were defined and  
111 reconstructed using probabilistic tractography. (b) The resulting connectivity matrices were then  
112 multiplied by connectivity matrices defining the connectivity of each vertex of the grey matter to the  
113 rest of the brain, creating a full connectivity blueprint (c) describing how each vertex is connected to  
114 each tract. (d) These blueprints can then be compared using the KL divergence as a comparative  
115 metric indicating how each vertex' connectivity fingerprint in one brain differs from that of each  
116 vertex in an other brain.

117

118

119

## 120 Results

121

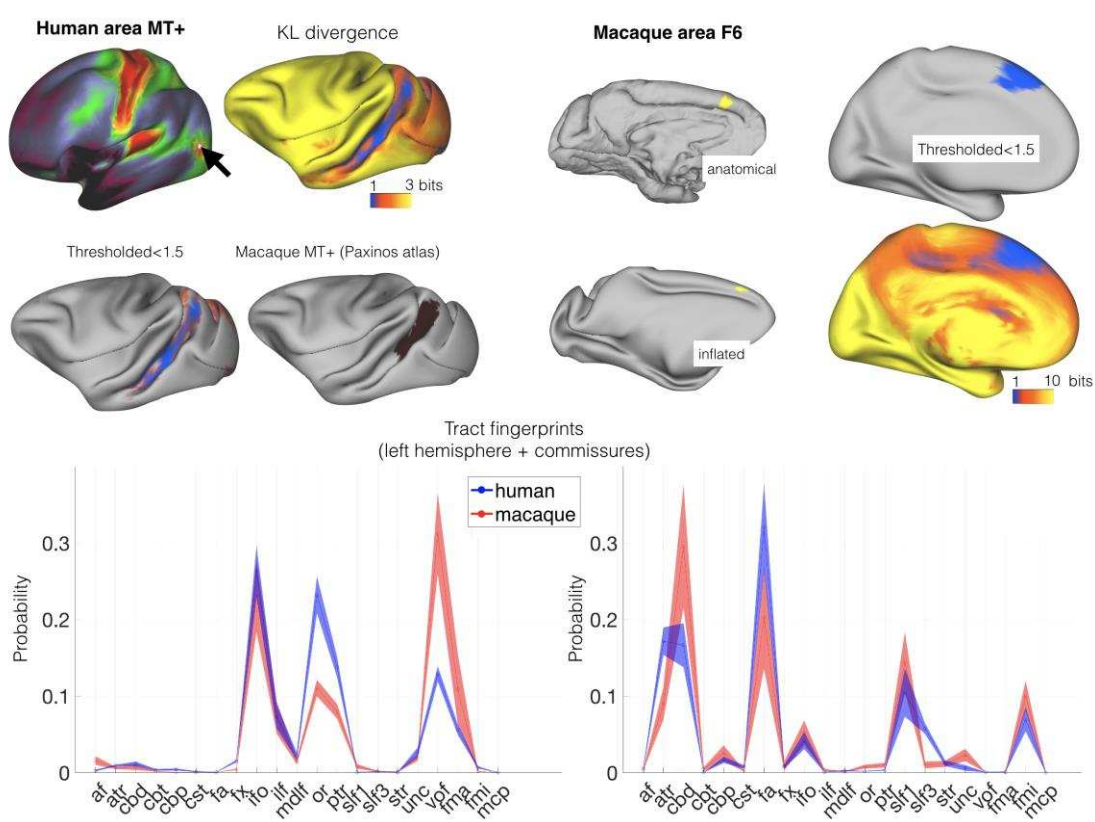
122 *Comparing connectivity blueprints can identify homologous areas across brains*

123

124 We first investigated whether the connectivity blueprints could be used to identify  
125 known homologs between the two species. Although the early visual areas are  
126 present in both humans and macaques, their location and the amount of cortical  
127 territory they occupy differs in the two species (Orban et al. 2004). A particularly  
128 challenging case is presented by areas sensitive to visual motion. The MT+ complex  
129 is located in the ventrolateral part of the posterior temporal cortex in the human  
130 brain (hMT+; Malikovic et al. (2015)), but is located more dorsally in the ventral bank  
131 of the posterior superior temporal sulcus in the macaque monkey (Paxinos et al.  
132 2000) (Fig. 2, left panel). hMT+ can be identified as a region of high myelin in the  
133 posterior temporal cortex that can be visualized using the ratio of T1- and T2-  
134 weighted MRI scans (Glasser and Van Essen 2011, Large et al. 2016). The peak of  
135 hMT+ is reached by tracts associated with the visual system such as the occipital  
136 radiations and the ventral occipital fascicle, but also by longitudinal tracts such as

137 the inferior longitudinal fascicle (Yeterian and Pandya 2010). We created a map of  
 138 the macaque cortex indicating how different each vertex' connectivity profile was to  
 139 that of a vertex in hMT+. This map showed the lowest divergence, i.e. highest  
 140 similarity, in the ventral bank of the macaque STS, as predicted from the macaque  
 141 cytoarchitectonic atlas. Thus, comparison of connectivity blueprints can identify  
 142 homologous areas across brains, even when their relative location has changed.  
 143

144 We next tested whether we could predict the location of the human pre-  
 145 supplementary motor area (pre-SMA), based on macaque area F6. It has been well-  
 146 established that these two regions share similar functions across the two species  
 147 (Nachev et al. 2008) and can be matched based on their connectivity profiles (Sallet  
 148 et al. 2013, Mars et al. 2016). Previous studies, however, matched the regions based  
 149 on the profile of functional connectivity with known homologous brain regions in  
 150 frontal and parietal cortex, rather than using white matter tracts that can potentially  
 151 be identified in all higher primates. We defined macaque area F6 based on the atlas  
 152 of Markov and colleagues (2011). Its connectivity fingerprint shows that it receives  
 153 widespread connections, including from the superior longitudinal fascicle, the  
 154 cingulum bundle, and the frontal aslant (cf. Thiebaut de Schotten et al. (2012)). We  
 155 determined the Kullback-Leibler (KL) divergence between the connectivity  
 156 fingerprint of F6 and that of each vertex of the human cortex. This map identified an  
 157 area of the human medial prefrontal cortex, anterior to the supplementary motor  
 158 area proper (Fig. 2, right panel) and consistent with previous localizations of this  
 159 area in the human (Nachev et al. 2008, Mars et al. 2016), as most similar to macaque  
 160 area F6. This result demonstrates that matching connectivity blueprints across  
 161 species can also be used to predict the location of areas outside early visual cortex.  
 162

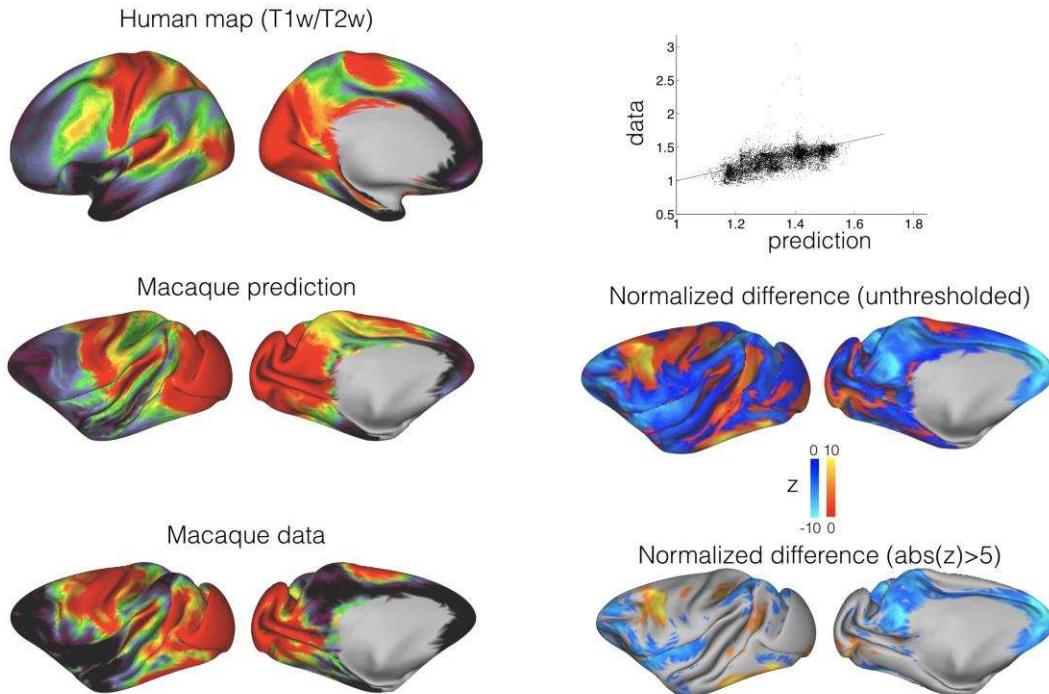


164 **Figure 2. Identifying areas across species. (left panel) MT+ complex.** Human MT+ can be defined as  
165 an area of high cortical myelin in the ventral occipitotemporal cortex (*top left*). Its connectivity  
166 fingerprint (shading indicates standard error) indicates strong projections from visual tracts such as  
167 the optic radiation, vertical occipital fascicle, inferior fronto-occipital fascicle, and inferior longitudinal  
168 fascicle (*bottom row*). According to previous work, macaque MT+ is located in the ventral bank of the  
169 superior temporal sulcus (*middle right*). Calculating the KL divergence of the connectivity fingerprint  
170 of human MT+ and the connectivity fingerprint of each macaque vertex (*top right*) shows the lowest  
171 divergence in the STS, with a thresholded image identifying the area predicted by previous work  
172 (*middle left*). **(right panel) Area F6.** Macaque area F6 (*left*) receives projections from, among others,  
173 the frontal aslant and the superior longitudinal fascicle (*bottom row*). Calculating the KL divergence of  
174 the connectivity fingerprint of macaque F6 and the connectivity fingerprint of each human vertex  
175 shows the lowest divergence on the medial wall, with a thresholded image identifying human pre-  
176 SMA (*right*).  
177  
178

179 *Connectivity blueprints can predict organization of the cortical surface across brains*  
180

181 As well as calculating divergence maps for a single vertex or a single area, the  
182 approach can be generalized to transform features of organization across the entire  
183 cortex between species. **One such map that is easily obtainable from neuroimaging**  
184 **is a T1/T2-weighted map, which has been suggested to partly reflect the presence**  
185 **of cortical myelin (Glasser et al. 2014).** T1/T2-weighted maps show a number of  
186 distinctive features across the human cortical hemisphere that are qualitatively  
187 similar to myelination maps, such as high values in primary sensory areas, low  
188 values in prefrontal and parietal association cortex, and intermediate values in  
189 frontal oculomotor areas. Using the connectivity blueprint as a reference space, we  
190 can transform a whole brain map from one species onto the other based on  
191 fingerprint similarities (see Methods). We used this approach to predict the **T1/T2-**  
192 **weighted map** of the macaque cortex based on the same map in humans (Fig. 3).  
193 The predicted map showed striking similarities to the actual macaque myelin map  
194 (Glasser et al. 2014), replicating the high myelin in the primary visual, auditory, and  
195 sensorimotor cortex and the low myelin in the prefrontal cortex.  
196

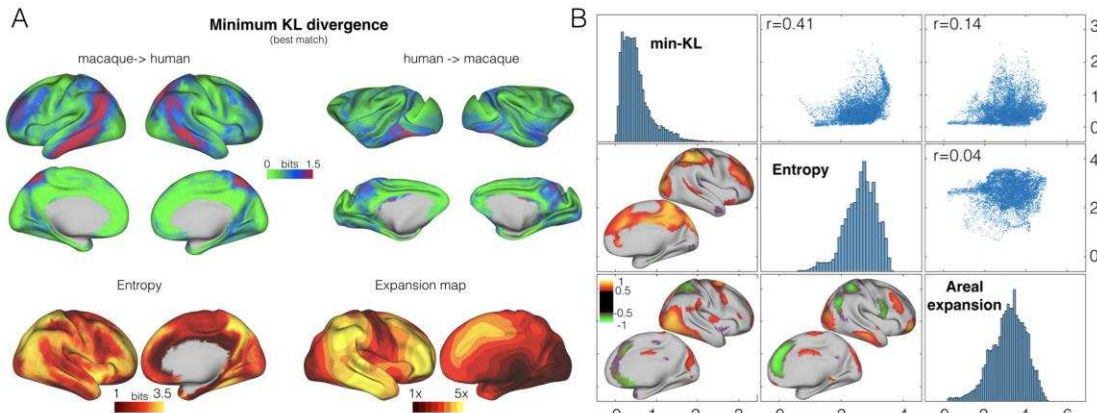
197 There are also areas in which the predicted macaque **T1/T2-weighted** map differs  
198 from the actual map. For instance, the predicted map showed an intermediate level  
199 of myelin in the macaque inferior parietal cortex, whereas in reality this is an area  
200 with low myelin content. Thus, there are parts of the cortex whose organization we  
201 could not predict well based on the connectivity blueprint. **While this could be due**  
202 **to limitations in the methods, it is noticeable that the poorer predictions are**  
203 **mostly located in the association cortex.** These are areas whose organization might  
204 be unique to one of the two brains studied. We therefore sought to quantify  
205 dissimilarity in connections between humans and macaques across the entire cortex.  
206



207  
 208 **Figure 3. Predicting macaque T1/T2-weighted map from the human map.** The connectivity blueprint  
 209 can be applied to use the human T1/T2-weighted map (*top left*) and predict the same map in the  
 210 macaque (*middle left*). The predicted macaque map shows strong similarity to an actual macaque  
 211 map based on 19 macaques from the Yerkes dataset (Donahue et al. *in press*). The scatter plot on  
 212 the top right shows how well the predicted map follows the data (straight line is  $y=x$ ). To assess the  
 213 variability in the predicted map, we calculated a distribution based on individual variability (using  
 214 all pairs of human/macaque datasets to build separate blueprints to drive the predictions). The  
 215 resulting distribution was compared to the measured map ( $Z=(\text{mean}-\text{data})/\text{std}$ ) (*middle right* and  
 216 *bottom right*). These assessments demonstrate that the predicted map shows striking similarities to  
 217 the actual map, but important differences are noticeable in part of the association cortex.  
 218  
 219

220 *Connectivity blueprints identify unique aspects of brain organization*  
 221

222 We investigated which parts of both the human and macaque brains are unique by  
 223 creating a map of the distance of each vertex to its closest match in the other  
 224 species. The greater the distance, the more likely this vertex has a connectivity  
 225 profile that is not represented in the other species; in other words, the more likely  
 226 this area has changed in its connectional organization since the last common  
 227 ancestor of human and macaque. The resulting connectional dissimilarity map  
 228 showed a large region of human inferior parietal and posterior temporal cortex,  
 229 precuneus, and to a lesser extent parts of the frontal cortex that could not be  
 230 predicted from any part of the macaque brain (Fig. 4, top panel). Importantly, the  
 231 between-species predictability does not correlate with any particular aspect of the  
 232 connectivity fingerprint, such as a map of the entropy of tract distribution (i.e.,  
 233 whether a region is reached strongly by few tracts or equally strongly by multiple  
 234 tracts) (Fig. 4). Similarly, the connectional dissimilarity map overlaps with, but is  
 235 different to a map of cortical expansion (Van Essen and Dierker 2007), indicating that  
 236 reorganization and expansion reflect separate aspects of brain reorganization (Fig.  
 237 4).



239

240

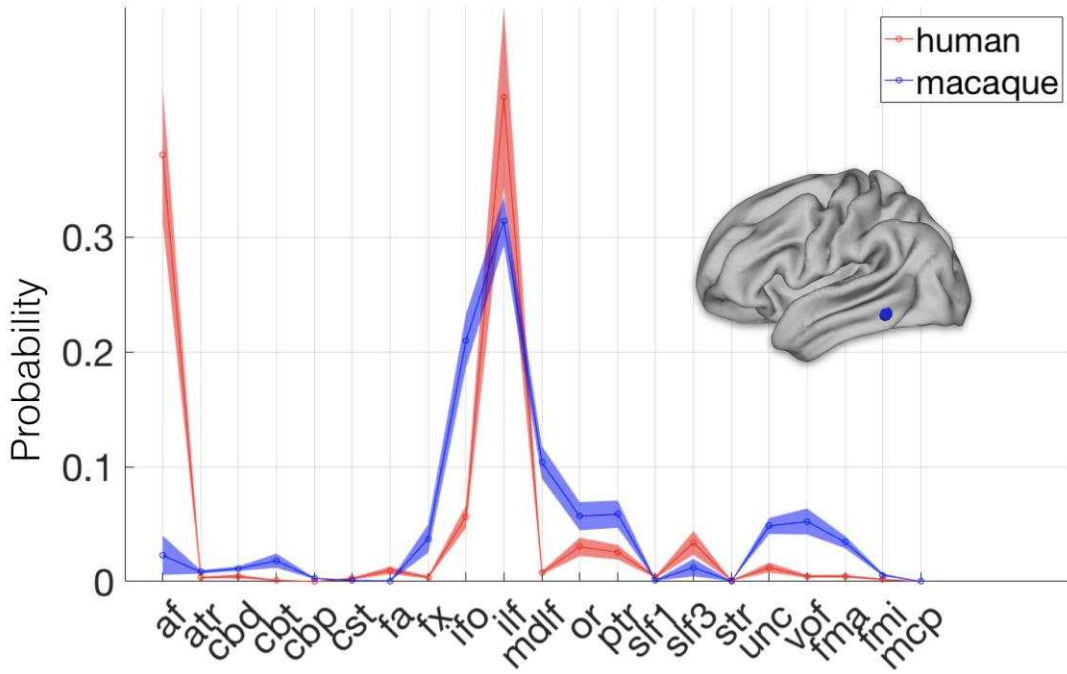
241 **Figure 4. Divergence map.** (A) A map of the minimum KL divergence of each vertex with all vertices in  
 242 the other species brain indicates which areas are least similar across the two brain (top panels). This  
 243 map can be compared with an entropy map showing the diversity of tracts reaching each vertex  
 244 (bottom left) and a landmark-based cortical expansion map (figure generated from data available from  
 245 the SUMSDB archive ([http://brainvis.wustl.edu/sumsdb/archive\\_index.html](http://brainvis.wustl.edu/sumsdb/archive_index.html)) (Van Essen and Dierker, 2007)  
 246 (bottom right). (B) We compared the KL divergence map with the entropy and expansion maps.  
 247 Diagonal shows the distribution of values of each map, upper right scatter plots show relationship  
 248 between all vertices of the pairs of maps; bottom left maps show the local correlations between  
 249 two maps.

250

251

252 The largest area in the human brain that has high connectional dissimilarity to the  
 253 macaque is a section of inferior parietal and posterior temporal cortex. This section  
 254 spans multiple cortical areas. We compared the fingerprint of the vertex with the  
 255 highest minimum KL divergence in the human brain, i.e., the vertex that has the least  
 256 similar match in the macaque, to the fingerprint of the most similar macaque  
 257 vertices (Fig. 5). This shows that this vertex is reached very prominently by the  
 258 arcuate fascicle (AF). The vertex is located in the posterior part of the temporal  
 259 cortex, an area that often shows activation in phonological or semantic tasks (Price  
 260 2000). Other parts of the cortex showing a high minimum divergence include the  
 261 anterior part of the human angular gyrus. The angular gyrus has also been suggested  
 262 to receive stronger AF connectivity than its proposed macaque homolog area PG  
 263 (Rilling et al. 2008). This part of angular gyrus has been shown to activate during  
 264 phoneme detection (Simon et al. 2002) and has stronger grey matter density in  
 265 bilinguals and adults who have learned to read compared to illiterates (Carreiras et  
 266 al. 2009). Consistent with this role, neurons in macaque area PG show visual  
 267 responses (Rozzi et al. 2008). Human angular gyrus receives input from the visual  
 268 word form area (Saygin et al. 2016). Together, these results are consistent with the  
 269 suggestion that the human brain contains areas with an organization not seen in the  
 270 macaque in areas recruited into the language system.

271



272  
 273 **Figure 5. Connectivity fingerprint of an area with high divergence.** The highlighted vertex on the  
 274 human cortical surface has a connectivity fingerprint dissimilar to any found in the macaque. The  
 275 vertex's connectivity fingerprint shows a much stronger influence of the arcuate fascicle even when  
 276 compared to the most similar vertices in the macaque (the blue line is the average of the top 1% most  
 277 similar macaque vertices). Shading indicates standard errors.

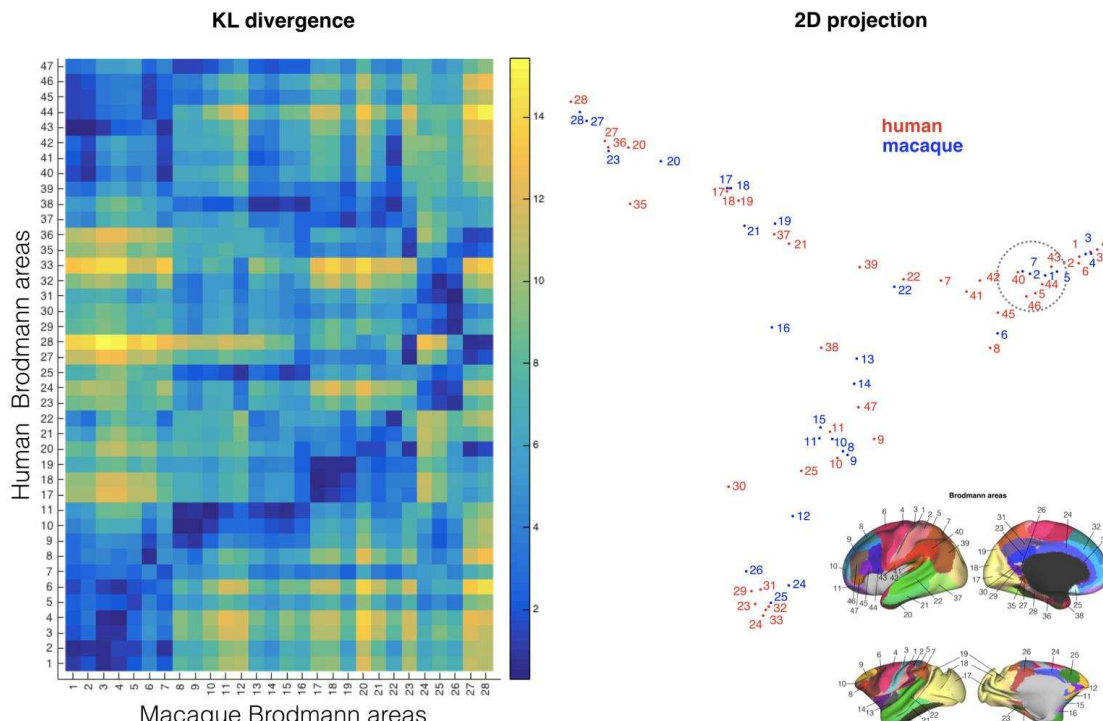
278  
 279  
 280 Other human areas that have a connectivity fingerprint that is poorly predicted  
 281 based on the macaque include the medial parietal cortex 7m and areas in the lateral  
 282 frontal cortex, including parts of dorsal prefrontal cortex. The medial parietal cortex  
 283 is reached by the first branch of the superior longitudinal fascicle and this  
 284 innervation seems stronger in the human brain. Based on shape analysis of  
 285 structural imaging data of the human and chimpanzee, Bruner and colleagues have  
 286 suggested that this area is preferentially expanded in the human brain (Bruner et al.  
 287 2017). The current results suggest that this expansion is accompanied by a change in  
 288 connectivity. In the frontal cortex, the forceps minor of the corpus callosum seems  
 289 stronger in the human than in the macaque, suggesting increased interhemispheric  
 290 connectivity within the prefrontal cortex in this species.

291  
 292 *Translation of cortical atlases based on the connectivity blueprint*  
 293

294 Another application of the blueprint approach to comparative anatomy is to use it to  
 295 translate between brain atlases. Comparative atlases of different species' brains are  
 296 rare in neuroscience, with most atlases focusing on a single species without explicit  
 297 comparisons to others. The blueprint approach, however, can be used to translate  
 298 between such different atlases. As an example we take the atlases of the human and  
 299 vervet monkey cortex produced by Brodmann (Brodmann 1905, Brodmann 1908)  
 300 which were converted to the human and macaque monkeys surface in the Caret  
 301 software (Van Essen et al. 2012). Brodmann labeled cytoarchitectonic areas in both  
 302 species, but the labeling was not meant to indicate homologies (Brodmann 1909,

303 Petrides et al. 2012). We calculated the divergence between Brodmann areas in the  
 304 two species and illustrated their similarities by projecting them to the same 2D space  
 305 using spectral reordering (Higham et al. 2007) (Fig. 6). At the gross level, this  
 306 showed that regions within similar cortical systems group together in the 2D  
 307 representation across the species. For instance, macaque primary visual areas 17  
 308 and 18 showed the smallest distance to human visual areas 18 and 19 and greatest  
 309 to areas 24 and 25 belonging to the cingulate cortex and early sensorimotor areas 3  
 310 and 4 that do not receive any direct visual projections. Similarly, areas 23, 24, and  
 311 25, all reached by the cingulum bundle, tended to cluster together.  
 312

313 The fact that the nomenclature of Brodmann's maps is not always consistent  
 314 between species is illustrated by monkey area 7 in the inferior parietal lobule (IPL).  
 315 This area showed smallest dissimilarity to human area 40 rather than human area 7.  
 316 This is consistent with the location of these areas, with human area 40 located on  
 317 the angular gyrus of the IPL and human area 7 belonging to the superior parietal  
 318 cortex (see highlighted area in Fig. 6). This result confirms earlier suggestions that  
 319 the IPL in the two species are indeed most similar to one another (cf. Mars et al.  
 320 (2011)) even though human IPL receives stronger arcuate connections, as  
 321 demonstrated above. In sum, these results show that our approach can be used to  
 322 translate existing cortical atlases across species, unifying previously diverse  
 323 anatomical endeavors.  
 324



325  
 326 **Figure 6. Comparing cortical atlases across species.** The connectivity blueprints can be used to  
 327 compare the connectivity fingerprint of cortical atlases of different species as illustrated here using  
 328 Brodmann's maps of the human and monkey (left). Using spectral clustering, the divergence of the  
 329 maps can be illustrated in a 2D representation, clustering together regions with the most similar  
 330 connectivity fingerprint (left). **Inset on the bottom right shows the atlas areas.**  
 331  
 332

333 **Discussion**

334

335 We have presented an approach to quantitatively compare cortical organization  
336 across species using their connectivity blueprint. We were able to predict known  
337 homologies between humans and macaques, such as the similarity of areas in visual  
338 cortex and the location of medial pre-SMA, but also to identify areas of diverging  
339 connectional reorganizations since the last common ancestor of humans and  
340 macaques. Moreover, we were able to provide a quantitative comparison of  
341 previously established atlases of the two species. We discuss the implications of this  
342 approach below, leaving a detailed discussion of its contribution to understanding  
343 macaque/human differences, including differences in lateralization and a further  
344 exploration of uniquely human aspects of temporal and frontal cortex organization,  
345 to a future communication.

346

347 Comparing the organization of the brains of related species is a fundamental  
348 challenge in neuroscience. Translational work relies on the assumption of  
349 evolutionary conservation, while evolutionary neuroscience aims to identify  
350 specializations explaining each species unique adaptations (Preuss 2001). Although  
351 cortical atlases are available for a number of model species, such as the macaque  
352 and marmoset monkeys, these are often not built with explicit comparisons in mind  
353 (Petrides et al. 2012). Moreover, the laborious and invasive nature of traditional  
354 cortical mapping studies means there are few maps even of our closest relatives,  
355 such as the great apes. The current work exploits the benefits of neuroimaging to  
356 quickly acquire detailed anatomical data from whole brains, both in-vivo or based on  
357 post-mortem preserved tissue. The simplicity of this approach means it can be  
358 widely applied and easily extended.

359

360 The current results demonstrate which parts of the human cortex have a large  
361 connectional dissimilarity to the macaque. Earlier direct comparisons between the  
362 human and macaque cortex used surface-based registration based on a few known  
363 homologous cortical landmarks to create an expansion map showing which areas in  
364 the human brain have disproportionately expanded compared to the macaque (Van  
365 Essen and Dierker 2007). This map showed areas of expansion in lateral prefrontal,  
366 inferior parietal, temporoparietal, and medial frontal cortex. Our connectional  
367 dissimilarity map is not an expansion map, but rather a map of connectional  
368 reorganization. Thus, the two maps describe separate aspects of cortical  
369 specialization, both of which are important in understanding what makes any one  
370 brain unique. Note, however, that the concept of the blueprint can also be used to  
371 create expansion maps that, rather than relying on morphological landmarks, use  
372 the blueprint as an anchor for measuring expansions. Similarly, a connectivity profile  
373 forms a different aspect of organization than the diversity of connections that a  
374 region receives, as indicated by our entropy map of tract distributions. There are  
375 different types of cortical organization that can result in a unique connectivity  
376 fingerprint, including invasion of new cortical territory as in the case of the arcuate  
377 and a change in the balance of connections due to strengthening of a particular  
378 connection (cf. Mars et al. (2018)). A future step will be to create comparative maps  
379 that specifically quantify these different types of cortical reorganization.

380 Our approach to comparative anatomy effectively defines a common space, the  
381 connectivity blueprint, for the brains of different species based on connections with  
382 white matter tracts. This approach was chosen because the body of these tracts can  
383 be reliably identified, ensuring that the common space is based on properties that  
384 are homologous. The tracts were established using recipes developed by the  
385 authors. Although in agreement with the published literature, this inevitably requires  
386 some judgment calls. An alternative would be to describe the tracts based on  
387 observer-independent approaches (O'Muircheartaigh and Jbabdi 2018), an approach  
388 that we aim to investigate in the future. However, if there is doubt regarding a  
389 particular tract, the current approach can also be used to test hypotheses regarding  
390 its course by testing the effect of various configurations on the similarity of the two  
391 brains. For example, one could search for a set of white matter tracts, a blueprint,  
392 that minimizes differences between cortical organization, under a parsimonious  
393 assumption of no connectional reorganization.

394  
395 The ultimate strength in this approach is in its flexibility. It can be used to predict  
396 features of cortical organization such as the **T1/T2-weighted** map we have shown  
397 here, but also to predict how specific systems translate between species (e.g., the  
398 multiple demand network, Mitchell et al. (2016)) or task-related activations when  
399 two species perform a similar task. Importantly, the approach can be generalized  
400 further by adapting the common space to include data from other modalities,  
401 including resting state functional MRI networks and maps of grey matter tissue  
402 properties such as myelin content or relative cortical thickness.

403  
404 In summary, a connectivity blueprint approach to comparative anatomy can allow us  
405 to bridge between cortical organizations in higher primates. Ultimately, this will lead  
406 to a reference template that represents common connectional organizations,  
407 deviations from which indicating species-specific specializations.

408  
409

## 410 **Methods**

411  
412

### 413 *Macaque data*

414

415 Four post-mortem macaque diffusion MRI datasets were used. Data from one male  
416 macaque (*Macaca fascicularis*) from a previous study (De Crespigny et al. 2005) were  
417 obtained and preprocessed as described in Jbabdi et al. (2013). Relevant imaging  
418 parameters were: 4.7T Oxford magnet equipped with BGA12 gradients; 3D  
419 segmented spin-echo EPI (430um isotropic resolution, 8 shots, TE = 33 ms, TR 350  
420 ms, 120 isotropically distributed diffusion directions, *b*-value = 8000 s/mm<sup>2</sup>.

421

422 Three additional macaque (*Macaca mulatta*) datasets (2 male) were acquired locally  
423 on a 7T magnet with an Agilent DirectDrive<sup>TM</sup> console (Agilent Technologies, Santa  
424 Clara, CA, USA) using a 2D diffusion-weighted spin-echo protocol with single line  
425 readout (DW-SEMS, TE/TR: 25 ms/10 s; matrix size: 128 x 128; resolution: 0.6 mm x  
426 0.6 mm; number of slices: 128; slice thickness: 0.6 mm). In these 3 monkeys, 9 non-

427 diffusion-weighted ( $b = 0$  s/mm $^2$ ) and 131 diffusion-weighted ( $b = 4000$  s/mm $^2$ )  
428 volumes were acquired with diffusion directions distributed over the whole sphere.  
429 The brains were soaked in PBS before scanning and placed in fomblin during the  
430 scan. The  $b=0$  images were averaged and spatial signal inhomogeneities were  
431 restored. Diffusion-weighted images were processed using FMRIB's Diffusion  
432 Toolbox, first to fit diffusion tensors and estimate the mean diffusivity and fractional  
433 anisotropy, followed by voxel-wise model fitting of diffusion orientations using  
434 BedpostX, using a crossing fiber model limited to three fiber directions (Behrens et  
435 al. 2007).

436  
437 *Human data*  
438

439 Human in-vivo data was obtained from the minimally pre-processed data provided  
440 by the Human Connectome Project ([www.humanconnectome.org](http://www.humanconnectome.org)) (Van Essen et al.  
441 2013). All acquisition parameters and processing pipelines are described in detail in  
442 Ugurbil et al. (2013), Sotropoulos et al. (2013), and Glasser et al. (2013). The  
443 diffusion MRI data consisted of three shells ( $b$ -values=1000, 2000, and 3000 s/mm $^2$ )  
444 with 270 diffusion directions equally spread amongst the shells, and six  $b=0$  s/mm $^2$   
445 acquisitions within each shell, with a spatial resolution of 1.25mm isotropic voxels.  
446 Ten subjects were chosen randomly from the Q900 data release. Data were pre-  
447 processed with the HCP pipeline, which involves susceptibility-induced distortion  
448 correction (Andersson et al. 2003) and eddy-current distortion and motion  
449 correction (Andersson and Sotropoulos 2016). A crossing fibre model adapted to  
450 multi-shell data (Jbabdi et al. 2012) was fitted to the data prior to tractography.

451  
452 *Surfaces*  
453

454 Models of the cortical surface were used for both humans and monkeys, including  
455 the pial surface and the white-gray matter interface. For humans, individual surface  
456 models were used, as provided through the HCP pipeline (Glasser et al. 2013), based  
457 on a Freesurfer surface reconstruction (Dale et al. 1999). For the macaque, we used  
458 surface reconstructions of one macaque with high quality structural MRI and  
459 nonlinearily (FSL's FNIRT) warped the other three macaque brains to enable using the  
460 same surface models in all four macaques. Macaque surfaces were then transformed  
461 to F99 standard space (Van Essen 2002) to facilitate the combination of tractography  
462 results. All the surfaces (macaque and human) were downsampled from ~32k to  
463 ~10k vertices prior to tractography analyses.

464  
465 *Extracting the anatomical blueprint*  
466

467 Probabilistic diffusion tractography (Behrens et al. 2007) as implemented in FSL's  
468 probtrackx2 was used to extract the anatomical blueprints of macaques and  
469 humans. We extended an automated tractography tool (autoPtx, De Groot et al.  
470 (2013)) to include a set of 39 major white matter bundles (18 on each hemisphere,  
471 and 3 cross-hemispheric pathways). Each bundle was reconstructed using a set of  
472 seed/inclusion/exclusion masks drawn in standard space (MNI152 for humans and  
473 F99 for macaques (Van Essen 2002)). **Tractography protocols for building the**

474 blueprints, code, and results are available for download from Gitlab at  
475 <https://git.fmrib.ox.ac.uk/rmars/comparing-connectivity-blueprints.git> (Jbabdi et  
476 al. 2018).

477

478 *Creating connectivity blueprints*

479

480 As shown in Figure 1, a connectivity blueprint consists of a (cortex) x (tracts) matrix  
481 where the tracts dimension is shared across both species. We build this matrix in  
482 two steps. First, we create a (cortex) x (whole brain) matrix by seeding probabilistic  
483 streamlines in standard space from every cortical vertex and recording the number  
484 of samples reaching each brain voxel (at 1mm/2mm resolution for F99  
485 macaque/MNI152 human). This is done using the “matrix2” mode in probtrackx2.  
486 Second, we multiplied the resulting matrix with a (brain) x (tracts) matrix, thus  
487 creating a (cortex) x (tracts) matrix. Rows of this matrix can be interpreted (once  
488 normalized to sum to one) as the probability distribution of streamlines from a given  
489 vertex to connect to each of the 39 tracts.

490

491 *Comparing connectivity blueprints*

492

493 We here introduce some mathematical notation: let  $M$  and  $H$  be the connectivity  
494 blueprint matrices for macaques and humans. For example,  $M_{ik}$  quantifies the  
495 probability that vertex  $i$  in the macaque cortex connects to tract  $k$ . We normalize the  
496 rows of  $M$  and  $H$  to sum to 1, thus turning the rows into a discrete probability  
497 distribution.

498

499 To compare the fingerprint of vertex  $i$  in macaque to vertex  $j$  in humans, we use the  
500 symmetric Kullback-Leibler (KL) divergence (Kullback and Leibler 1951) as a  
501 dissimilarity measure:

502

$$503 D_{ij} = \sum_k M_{ik} \log_2 \frac{M_{ik}}{H_{jk}} + \sum_k H_{jk} \log_2 \frac{H_{jk}}{M_{ik}}$$

504 Similarly, the same distance measure can be used to compare two vertices within  
505 species.

506

507 *Mapping between species*

508

509 The similarity matrix calculated above can be used to transform a map from one  
510 species to the other using distance weighted interpolation (as done to map the  
511 myelin map from human to macaque in the Results section).

512

513 Given a map on the human cortex  $h_i$  where  $i$  indexes vertices, we obtain a  
514 transformed macaque map  $m$  as follows:

$$515 m_j = \frac{\sum D_{ji}^\gamma h_i}{\sum D_{ji}^\gamma}$$

516 where we used  $\gamma = -4$ .

517

518

519 **Acknowledgements**

520

521 This work was supported by the Biotechnology and Biological Sciences Research  
522 Council UK [BB/N019814/1]; the Netherlands Organization for Scientific Research  
523 NWO [452-13-015]; Cancer Research UK [C5255/A15935]; the Wellcome Trust  
524 [105651/Z/14/Z]; and the Medical Research Council UK [MR/L009013/1]. The  
525 Wellcome Centre for Integrative Neuroimaging is supported by core funding from  
526 the Wellcome Trust [203139/Z/16/Z]. **RBM would like to thank Hiromasa Takemura**  
527 **for helpful discussion regarding VOF. The work leading to the macaque T1/T2-**  
528 **weighted “myelin map” was supported in part by National Institutes of Health**  
529 **Grants P01AG026423 and the Yerkes National Primate Research Center base grant**  
530 **(Office of Research Infrastructure Programs; grant OD P51OD11132). We thank**  
531 **Nicole Eichert for help on aspects of surface processing.**

532

533

534 **Competition financial interests**

535

536 None.

537

538

539 **References**

540

541 Andersson JLR, Skare S and Ashburner J (2003) How to correct susceptibility distortions in spin-echo  
542 echo-planar images: Application to diffusion tensor imaging. *Neuroimage* 20: 870-888.

543 Andersson JLR and Sotiroopoulos SN (2016) An integrated approach to correction for off-resonance  
544 effects and subject movement in diffusion MRI imaging. *Neuroimage* 125: 1063-1078.

545 Behrens TE, Berg HJ, Jbabdi S, Rushworth MF and Woolrich MW (2007) Probabilistic diffusion  
546 tractography with multiple fibre orientations: What can we gain? *Neuroimage* 34: 144-155.

547 Brodmann K (1905) Beiträge zur histologischen Lokalisation der Grosshirnrinde. III. Die Rindenfelder  
548 der niederen Affen. *J Psychol Neurol* 4: 177-226.

549 Brodmann K (1908) Beiträge zur histologischen Lokalisation der Grosshirnrinde. VI. Die  
550 Cortexgliederung des Menschen. *J Psychol Neurol* 10: 231-246.

551 Brodmann K (1909) *Vergleichende Lokalisationslehre der Grosshirnrinde in ihren Prinzipien*  
552 *dargestellt auf Grund des Zellenbaues*. Leipzig: Verlag.

553 Bruner E, Preuss TM, Chen X and Rilling JK (2017) Evidence for expansion of the precuneus in human  
554 evolution. *Brain Struct Funct* 222: 1053-1060.

555 Carreiras M, Seghier ML, Baquero S, Eastévez A, Lozano AM, Devlin JT and Price CJ (2009) An  
556 anatomical signature for literacy. *Nature* 461: 983-986.

557 Dale AM, Fischl B and Sereno MI (1999) Cortical surface-based analysis. I. Segmentation and surface  
558 reconstruction. *Neuroimage* 9: 179-194.

559 De Crespigny AJ, D'Arceuil HE, Maynard KL, He J, McAuliffe D, Norbush A, Sehgal PK, Hamberg L,  
560 Hunter G, Budzik RF, Putman CM and Gonzalez RG (2005) Acute studies of a new primate  
561 model of reversible middle cerebral artery occlusion. *J Stroke Cerebrovasc Dis* 14: 80-87.

562 De Groot M, Vernooy MW, Klein S, Ikram MA, Vos FM, Smith SM, Niessen WJ and Andersson JLR  
563 (2013) Improving alignment in tract-based spatial statistics: Evaluation and optimization of  
564 image registration. *Neuroimage*.

565 Donahue CJ, Glasser MF, Preuss TM, Rilling JK and Van Essen DC (in press) A quantitative assessment  
566 of prefrontal cortex in humans relative to nonhuman primates. *Proc Natl Acad Sci USA*.

567 Glasser MF, Goyal MS, Preuss TM, Raichle ME and Van Essen DC (2014) Trends and properties of  
568 human cerebral cortex: correlations with cortical myelin content. *Neuroimage* 93 Pt 2: 165-  
569 175.

570 Glasser MF, Sotiroopoulos SN, Wilson JA, Coalson TS, Fischl JR, Andersson JL, Xu J, Jbabdi S, Webster M,  
571 Polimeni JR, Van Essen DC and Jenkinson M (2013) The minimal preprocessing pipelines for  
572 the Human Connectome Project. *NeuroImage* 80: 105-124.

573 Glasser MF and Van Essen DC (2011) Mapping human cortical areas in vivo based on myelin content  
574 as revealed by T1- and T2-weighted MRI. *J Neurosci* 31: 11597-11616.

575 Hecht EE, Gutman DA, Preuss TM, Sanchez MM, Parr LA and Rilling JK (2013) Process versus product  
576 in social learning: Comparative diffusion tensor imaging of neural systems for action  
577 execution-observation matching in macaque, chimpanzees, and humans. *Cereb Cortex* 23:  
578 1014-1024.

579 Higham DJ, Kalna G and Kibble M (2007) Spectral clustering and its use in bioinformatics. *J Computat  
580 Appl Math* 204: 25-37.

581 Jbabdi S, Lehmann JF, Haber Sn and Behrens TE (2013) Human and monkey ventral prefrontal fibers  
582 use the same organizational principles to reach their targets: Tracing versus tractography. *J  
583 Neurosci* 33: 3190-3201.

584 Jbabdi S, Sotiroopoulos SN and Mars RB (2018). comparing-connectivity-blueprints,  
585 <https://git.fmrib.ox.ac.uk/rmars/comparing-connectivity-blueprints.git>,  
586 7f4a8b6.

587 Jbabdi S, Sotiroopoulos SN, Savio AM, Grana M and Behrens TEJ (2012) Model-based analysis of  
588 multishell diffusion MR data for tractography: How to get over fitting problems. *Magn Res  
589 Med* 68: 1846-1855.

590 Kullback S and Leibler RA (1951) On information and sufficiency. *Ann Math Statist* 22: 79-86.

591 Large I, Bridge H, Ahmed B, Clare S, Kolasinski J, Lam WW, Miller KL, Dybry TB, Parker AJ, Smith JET,  
592 Daubney G, Sallet J, Bell AH and Krug K (2016) Individual differences in the alignment of  
593 structural and functional markers of the V5/MT complex in primates. *Cereb Cortex* 26: 3928-  
594 3944.

595 Malikovic A, Amunts K, Schleicher A, Mohlberg H, Kujovic M, Palomero-Gallagher N, Eickhoff SB and  
596 Zilles K (2015) Cytoarchitecture of the human lateral occipital cortex: mapping of two  
597 extrastriate areas hOc4la and hOc4lp.

598 Markov NT, Misery P, Falchier A, Lamy C, Vezoli J, Quilodran R, Gariel MA, Giroud P, Ercsey-Ravadz M,  
599 Pilaz LJ, Huissoud C, Barone P, Dehay C, Toroczkai Z, Van Essen DC, Kennedy H and Knoblauch  
600 K (2011) Weight consistency specifies regularities of macaque cortical networks. *Cereb  
601 Cortex* 21: 1254-1272.

602 Mars RB, Eichert N, Jbabdi S, Verhagen L and Rushworth MFS (2018) Connectivity and the search for  
603 specializations in the language-capable brain. *Curr Opin Behav Sci* 21: 19-26.

604 Mars RB, Jbabdi S, Sallet J, O'Reilly JX, Croxson PL, Olivier E, Noonan MP, Bergmann C, Mitchell AS,  
605 Baxter MG, Behrens TE, Johansen-Berg H, Tomassini V, Miller KL and Rushworth MF (2011)  
606 Diffusion-weighted imaging tractography-based parcellation of the human parietal cortex  
607 and comparison with human and macaque resting-state functional connectivity. *J Neurosci*  
608 31: 4087-4100.

609 Mars RB, Verhagen L, Gladwin TE, Neubert FX, Sallet J and Rushworth MFS (2016) Comparing brains  
610 by matching connectivity profiles. *Neurosci Biobehav Rev* 60: 90-97.

611 Mitchell DJ, Bell AH, Buckley MJ, Mitchell AC, Sallet J and Duncan J (2016) A putative multiple-demand  
612 system in the macaque brain. *J Neurosci* 36: 8574-8585.

613 Nachev P, Kennard C and Musain M (2008) Functional role of the supplementary and pre-  
614 supplementary motor areas. *Nat Rev Neurosci* 9: 856-869.

615 O'Muircheartaigh J and Jbabdi S (2018) Concurrent white matter bundles and grey matter networks  
616 using independent component analysis. *NeuroImage* 170: 296-306.

617 Orban GA, Van Essen D and VanDuffel W (2004) Comparative mapping of higher visual area in  
618 monkeys and humans. *Trends Cogn Sci* 8: 315-324.

619 Passingham RE, Stephan KE and Kotter R (2002) The anatomical basis of functional localization in the  
620 cortex. *Nat Rev Neurosci* 3: 606-616.

621 Paxinos G, Huang XF and Toga AW (2000) *The rhesus monkey brain in stereotaxic coordinates*. San  
622 Diego: Academic Press.

623 Petrides M, Tomaiuolo F, Yeterian EH and Pandya DN (2012) The prefrontal cortex: comparative  
624 architectonic organization in the human and the macaque monkey brains. *Cortex* 48: 46-57.

625 Preuss TM (2001) The discovery of cerebral diversity: An unwelcome scientific revolution. In:  
626 *Evolutionary anatomy of primate cerebral cortex*. D. Falk and K. R. Gibson (eds.). Cambridge:  
627 Cambridge University Press. pp. 138-164.

628 Price CJ (2000) The anatomy of language: Contributions from functional neuroimaging. *J Anat* 197:  
629 335-359.

630 Rilling JK, Glasser MF, Preuss TM, Ma X, Zhao T, Hu X and Behrens TEJ (2008) The evolution of the  
631 arcuate fasciculus revealed with comparative DTI. *Nat Neurosci* 11: 426-428.

632 Rozzi S, Ferrari PF, Bonini L, Rizzolatti G and Fogassi L (2008) Functional organization of inferior  
633 parietal lobule convexity in the macaque monkey: Electrophysiological characterization of  
634 motor, sensory and mirror responses and their correlation with cytoarchitectonic areas. *Eur J  
635 Neurosci* 28: 1569-1588.

636 Sallet J, Mars RB, Noonan MP, Neubert FX, Jbabdi S, O'Reilly JX, Filippini N, Thomas AG and Rushworth  
637 MF (2013) The organization of dorsal frontal cortex in humans and macaques. *J Neurosci* 33:  
638 12255-12274.

639 Saygin ZM, Osher DE, Norton ES, Youssoufian DA, Beach SD, Feather J, Gaab N, Gabrieli JDE and  
640 Kanwisher N (2016) Connectivity precedes function in the development of the visual word  
641 form area. *Nat Neurosci* 19: 1250-1255.

642 Simon O, Mangin JF, Cohen L, Le Bihan D and Dehaene S (2002) Topographical layout of hand, eye,  
643 calculation, and language-related areas in the human parietal lobule. *Neuron* 33: 475-487.

644 Sotiroopoulos SN, Jbabdi S, Xu J, Andersson JL, Moeller S, Auerbach EJ, Glasser MF, Hernandez M,  
645 Sapiro G, Jenkinson M, Feinberg DA, Yacoub E, Lenglet C, Van Essen DC, Ugurbil K, Behrens  
646 TE and Consortium W-MH (2013) Advances in diffusion MRI acquisition and processing in the  
647 Human Connectome Project. *NeuroImage* 80: 125-143.

648 Thiebaut de Schotten M, Dell'Acqua F, Valabregue R and Catani M (2012) Monkey to human  
649 comparative anatomy of the frontal lobe association tracts. *Cortex* 48: 82-96.

650 Ugurbil K, Xu J, Auerbach EJ, Moeller S, Vu AT, Duarte-Carvajalino JM, Lenglet C, Wu X, Schmitter S,  
651 Van de Moortele PF, Strupp J, Sapiro G, De Martino F, Wang D, Harel N, Garwood M, Chen L,  
652 Feinberg DA, Smith SM, Miller KL, Sotiroopoulos SN, Jbabdi S, Andersson JLR, Behrens TEJ,  
653 Glasser MF, Van Essen DC, Yacoub E and Consortium W-MH (2013) Pushing spatial and  
654 temporal resolution for functional and diffusion MRI in the Human Connectome Project.  
655 *NeuroImage* 80: 80-104.

656 Van Essen DC (2002) Windows on the brain: The emerging role of atlases and databases in  
657 neuroscience. *Curr Opin Neurobiol* 12: 574-579.

658 Van Essen DC and Dierker DL (2007) Surface-based and probabilistic atlases of primate cerebral  
659 cortex. *Neuron* 56: 209-225.

660 Van Essen DC, Glasser MF, Dierker DL and Harwell J (2012) Cortical parcellations of the macaque  
661 monkey analyzed on surface-based atlases. *Cereb Cortex* 22: 2227-2240.

662 Van Essen DC, Smith SM, Barch DM, Behrens TE, Yacoub E, Ugurbil K and Consortium W-MH (2013)  
663 The WU-Minn Human Connectome Project: An overview. *NeuroImage* 80: 62-79.

664 Yeterian EH and Pandya DN (2010) Fiber pathways and cortical connections of preoccipital areas in  
665 rhesus monkeys. *J Comp Neurol* 518: 3725-3751.

666

667